NASA-CR-200751

Topography and Surface Change Award NAG 5-2987:
"Scale - space (wavelet) analysis of topography, and its use in understanding the evolution of erosional fronts and escarpments bounding continental plateaus", Jeffrey K. Weissel (PI) and Michele A. Seidl (CoI).

PROGRESS REPORT Year I (07/01/1995 - 06/30/1996)

Introduction

The main effort during the first year of the above referenced NASA/MTPE Topography and Surface Change award has been on finalizing the theory for multiresolution analysis of topographic slope and curvature, finishing the computer software for doing the analyses, and conducting tests with synthetic data as well as digital elevation models (DEMs). The methodology and some applications are described in a manuscript entitled "Multiresolution analysis of topographic slope and curvature with application to landscape evolution" which will be submitted for publication this spring (*Weissel and Stark*, in prep.). Portions of this work will be presented at the 1996 Spring AGU Meeting in Baltimore, and at the West Pacific Geophysics Meeting (WPGM) in Brisbane, Australia next July (see attached abstracts by *Stark and Weissel* and by *Stark, Hovius, and Weissel*).

Main Scientific Results

We would like to highlight three of the most important results stemming from the research so far. While these results are described some of the details of new wavelet-based multiresolution estimation (MRE) technique will be outlined.

1. Determination of topographic slope and curvature from noise-contaminated DEMs for assessment of landscape slope stability

Slope stability in many environments is often assessed using local topographic slope and/or shape (curvature) criteria. However, we face a major problem in attempting to apply these criteria because the various DEMs we would use are contaminated by spatially-varying noise, error and artifact. Different DEMs are affected by different sources of error. For example, the accuracy of DEMs derived from radar interferometry is thought to depend on local relief, with uncertainties of ± 1-2 m being characteristic of locally "smooth" terrain and larger uncertainties ± 3-5 m characteristic of "rough" terrain. In addition, heights obtained from radar interferometry are biased upward for vegetated landscapes. The presence of spatially-varying noise makes it difficult to obtain the accurate, high-resolution estimates of topographic slope and curvature required for slope stability assessment. Traditional Fourier-based techniques are not effective for separating topographic "signal" from noise when the noise is spatially inhomogeneous (i.e., non-stationary). Similarly, standard finite differencing techniques serve to enhance noise when used in these situations (as discussed below).

Wavelet-based analysis techniques seem to provide a solution to the spatially inhomogeneous noise problem because:

1. Natural topography possesses length-scaling properties different from the contaminating noise.
2. Scaling properties of the topography dominate those of the noise over some finite, intermediate range of length scales.
3. Wavelet-based techniques determine the **local** scaling properties (as opposed to global scaling properties) as discussed later.

It is therefore feasible to separate signal from noise locally by extrapolating the scaling properties determined at a coarse scale, where the topographic signal dominates, to a finer scale in order to obtain more accurate, high-resolution estimates of topographic slope and curvature.

To illustrate the noise effects briefly, consider the problem of determining topographic slope for three 1° squares of DMA DTED topography from northern Somalia. The north-south component of topographic slope which is shown as a grey scale image in **Fig. 1** was determined by first differences at the grid interval. This image reveals many of the noise and artifact problems in the DTED data (*Weissel et al.*, 1994), and it serves to demonstrate that standard finite difference techniques for determining derivatives like slope and curvature amplify short-wavelength noise and artifact. A simple illustration of how multiresolution methods deal with noise problems is shown in **Fig. 2**, which depicts "noisy" topography data across a sloping edge. We want to locate the edge, specify its width, and determine its slope accurately. The fundamental problem is finding the right **width** (or length-scale) operator to use - too long and too short give incorrect answers. The best approach is to estimate slope at **all positions** using operators that span **a wide range** of length scales, and this is the heart of wavelet methods.

A short review the basics of wavelet-based techniques is appropriate here: The wavelet transform (WT for short) of a two-dimensional function $h(x)$ with respect to a particular wavelet family $\psi_{\theta,a,b}$ is given as the inner product ($\approx$ correlation function) between h and $\psi_{\theta,a,b}$:

$$\mathcal{W}_\psi(h;\, \theta,\, a,\, b) = \int_{x\in\mathbb{R}_2} h(x)\, \bar{\psi}\left(\Omega^{-1}(\theta)\, \frac{x-b}{a}\right) dx \tag{1}$$

where $a \in \mathbb{R}_+$ is length-scale (or, more correctly) dilation, $b \in \mathbb{R}_2$ is position, and θ is the polarization angle. Eqn. (1) shows that the wavelet family $\psi_{\theta,a,b}$ is formed by shifting, stretching, and rotating a "parent" wavelet $\psi(x)$. Not any wiggly function can be called a wavelet. There is an admissibility condition, which essentially says that wavelets have zero mean. Wavelets should also be well-localized (or compact) in both the space and wavenumber domains.

The choice of wavelet depends on what the analysis objectives are. In our case, we want to estimate derivatives like slope and curvature from gridded topography. The best approach is to use wavelets that are derivatives of smoothing functions like the splines or the Gaussian. During the first year of NASA support, *Weissel and Stark* (in prep.) have developed an algebra of spline- and Gaussian-derivative wavelets, and related these to finite differences operators commonly used to estimate derivatives of discrete data numerically. This new work along with some applications will be submitted for publication this Spring. At the 1996 Spring AGU meeting we will present details of the methodology and discuss applications to slope stability assessment using DEMs from from a number of different areas around the world (see *Stark and Weissel* Spring AGU abstract).

2. Determining the scaling properties of topography

One of the most important applications of wavelet-based methods is, as stated above, the estimation of local length scaling properties. Topographic surfaces possess length scaling properties across a wide range in wavelengths as indicated, for example, by the power law decay in the power spectrum of topographic profiles and surfaces (see e.g., *Weissel et al.*, 1994). We must remember, however, that only a restricted range of length scales are available to us for examination in DEMs. Normally the minimum length scale is the gridding interval. Scaling behavior at shorter length scales cannot be detected unless a DEM with finer resolution is used.

Probably the best way to to envisage local scaling behavior is to consider a Taylor expansion of a signal $h(x)$ about a point x_0 at "resolution" or length scale l. We assume that the signal possesses a "singularity" at x_0 in the sense that an extra term dependent on the local Hölder exponent is required in the Taylor series

$$h(x_0 + l) = h(x_0) + l \cdot h^{(1)}(x_0) + \cdots + (l^n/n!) \cdot h^{(n)}(x_0) + C \cdot |l|^{\alpha(x_0)} \tag{2}$$

where (n) denotes the n-th derivative of h. As $l \to 0$, we can say that a local scaling exponent (or "singularity" of strength) α with a value $n < \alpha(x_0) < n + 1$ occurs at the point x_0.

We can rewrite (2) more compactly as

$$h(x_0 + l) - P_n(l) = C \cdot |l|^{\alpha(x_0)} \tag{3}$$

where $P_n(l)$ is a polynomial of order n in l. Now, if we extend the admissibility condition (2) to say that the analyzing wavelet must have $n + 1$ vanishing moments, we now have

$$\int_{-\infty}^{\infty} x^m \, \psi(x) \, dx \;=\; 0, \;\; \text{for } m \;=\; 0, \cdots, n \,. \tag{4}$$

Under this condition the WT of h will be "blind" to the regular (polynomial) part of the signal, and thus (1) will behave like

$$|\mathcal{W}_\psi(h;\, a,\, x_0)| \;\sim\; a^{\alpha(x_0)}, \;\text{ as a} \to\; 0\,. \tag{5}$$

Thus, the amplitude of the wavelet transform at x_0 decays downscale according to the singularity strength $\alpha(x_0)$ which can (in principle) be determined from the slope of a logarithmic-scale plot of WT amplitude against a.

Three different types of scaling behavior can be distinguished:

1. Signals might be **singular almost everywhere** with a constant singularity strength H. This case is called **simple scaling**. When $0 < H < 1$, all derivative terms in the Taylor series expansion (2) are zero, and (3) becomes

$$|h(x_0 \,+\, l) \;-\; h(x_0)| \;\sim\; |l|^H \;. \tag{6}$$

   Fractional Brownian (fBm) profiles and surfaces have this kind of scaling property. Many people still believe that topography is simple scaling, but this belief is commonly based on techniques (spectral analysis, structure functions) that yield only global or average scaling information. In practice, however, wavelet analysis of single realizations of fractional Brownian profiles yield a range in scaling exponents with an average close to the nominal value of H. We have found that this spurious multiscaling arises because of statistical fluctuations in single realizations of fBm, and it can be reduced (i.e., the histogram of exponents narrowed) but not eliminated if the Hilbert transform of the WT is determined, and the scaling analysis done on the analytic function rather than the WT amplitude as in (5).

2. True **multiscaling behavior** occurs where the signal is singular almost everywhere, and singularity strength or local scaling exponent varies over a range of values (say, $\alpha_{min} < \alpha(x) < \alpha_{max}$) that are interwoven on fractal subsets of the total (Euclidian) support of the surface or profile. Multiscaling analysis consists of finding the range of singularity strengths present in a given signal sample, then determining the Hausdorff (fractal) dimension $D(\alpha)$ of the subset of points associated with each singularity strength α, i.e., finding

$$D(\alpha) \;=\; dim\{x \,|\, \alpha(x) \;=\; \alpha\}. \tag{7}$$

   A plot of $D(\alpha)$ versus α yields the required singularity spectrum, as shown below (**Fig. 3**).

3. **Pseudo-multiscaling behavior** occurs in two ways. The first is the spurious multiscaling that arises from wavelet analysis of synthetic monofractals like fBm as discussed above. This raises the unlikely possibility that topography is simple-scaling but our wavelet-based methodology makes it appear multiscaling. One reason for this is that topography is not an outcome of a stochastic process (like fBm) which would generate a monofractal, and thus there is no reason to expect that the variation in scaling exponents determined in the analysis reflects statistical fluctuations. The second case of pseudo-multiscaling accepts the measured variation in scaling exponents as real, but questions whether these are supported on fractal sets as required for true multiscaling behavior. **This seems to be the case with topography**, as our investigation of scaling properties shows (**Figs. 3 and 4**).

We illustrate our results on topography scaling properties using a topographic profile made from airborne laser altimeter measurements at Walnut Gulch, AZ (**Figs. 3 and 4**). The heights obtained from laser altimetry are highly accurate, especially in this semi-arid terrain. The singularity spectrum $D(\alpha)$ is plotted against singularity strength (or scaling exponent) α in **Fig. 3** both for the Walnut Gulch altimetry profile and a known synthetic multiscaling profile made from a multiplicative binomial cascade. **The main feature** of the Walnut Gulch singularity spectrum **is the presence of scaling exponents** > 1. This means that certain parts of the topographic profile are continuous in the first derivative, and singular in the second derivative. This result casts doubt upon fractal models for topography, especially fBm analogues of topography, because these have scaling exponents $0 < \alpha < 1$. To reinforce this new result, **Fig. 4** graphs local scaling exponent α against position x_O or b along a portion of the Walnut Gulch altimetry profile. The solid curve at the bottom oscillating about $\alpha = 0.5$ denotes scaling exponents determined using a first-derivative Gaussian wavelet, while the broken and dotted curves oscillating at 1 and above on the right were determined using second- and fourth-derivative Gaussian wavelets, respectively. As expected from (4), the first-derivative wavelet is unable to detect singularities of strength ≥ 1. Notice the sharp transition from scaling exponents $0.5 \lesssim \alpha \lesssim 0.8$ to scaling exponents ≥ 1 at position 9200. The cause for this abrupt transition in scaling behavior is not clear at present, but it is clearly important and worthy of future study. Our favored explanation at this stage is that different parts of the landscape which originate in different ways might display scaling behavior over different ranges of length scale. Parts of the landscape whose scaling behavior occurs at scales that are short compared to the gridding interval would appear "smooth" over the range of length scales treated in the analysis.

3. Linking size - frequency scaling of landslides with the length-scaling properties of topography

Mapping of landslide scars from airphotos of the Southern Alps of New Zealand has revealed that this mass-wasting process is scale invariant up to a length scale of about 1 km (*Hovius, Stark and Allen*, submitted). The global scaling properties of the terrain were determined from our wavelet-based MRE analysis using a DEM provided by New Zealand workers. We found that the scaling exponent of the power law describing the landslide size - frequency distribution $\beta \approx -1.16$ is about equal to the exponent describing the overall length scaling of topography $\alpha \approx 1.1$ minus 2. In other words the landslide scaling exponent is approximately equal to that of the second derivative of topography, i.e., its curvature. The scaling linkage suggests that topographic curvature is the rate determining parameter for hillslope failure in the Southern Alps of New Zealand, and not hillslope gradient magnitude (see *Stark, Hovius, and Weissel* WPGM abstract).

Other Related Results

New results stemming from the 1993 Australian AIRSAR/TOPSAR deployment and related field observations have been prepared for publication. A manuscript by *Seidl, Weissel, and Pratson* (in press) exploring the development of the erosional escarpment along the southeastern rifted margin of Australia will be published shortly in *Basin Research*. The key result of that work is that the gorge-head form of erosional escarpment appears to have propagated inland up the drainage system of the Macleay River at an average rate of 2 km/my since formation of the margin 80 - 100 my ago. In November 1995 one of us (JKW) attended a workshop in Sydney, Australia to discuss results of the 1993 Australian AIRSAR/TOPSAR campaign. This was the first opportunity to present DEMs from radar interferometry and related AIRSAR polarimetry data obtained from sites across, above, and below the erosional escarpment of the New England section of the southeastern Australian margin. Those preliminary results are described in a meeting proceedings report (*Weissel*, in press), whose publication is expected shortly.

References

Hovius, N., C.P. Stark, and P.A. Allen, Sediment flux from a mountain belt derived by landslide mapping, submitted to *Nature.*

Seidl, M.A., J.K. Weissel, and L.F. Pratson, Kinematics and pattern of escarpment retreat across the rifted continental margin of southeastern Australia, *Basin Research*, in press.

Stark, C.P., and J.K. Weissel, Using wavelets to determine slope stability from Digital Elevation Models (DEMs), Session T03 -Topography and Land Surface Processes, AGU Spring Meeting, 1996, (**see attached abstract**).

Stark, C.P., N. Hovius, and J.K. Weissel, The linked scaling of landsliding and topography in the Southern Alps, NZ, WPGM July 1996, (**see attached abstract**).

Weissel, J.K., Airborne radar investigation of escarpment erosion across the New England section of the southeast Australian continental margin, *Proc. AIRSAR Australia 1993 Workshop*, UNSW, Australia, in press.

Weissel, J.K., and C.P. Stark, Multiresolution analysis of topographic slope and curvature with application to landscape evolution, in prep.

Weissel, J.K., L.F. Pratson, and A. Malinverno, The length-scaling properties of topography, *J. Geophys. Res., 99*, 13,997-14,012, 1994.

Fig. 1. North-south topographic gradient for three 1° squares of DMA 3 arc sec. topography from Somalia presented as grey-scale image. Notice the spatially inhomogeneous field of noise and artifact that is amplified by determining the gradient at the grid interval of the data.

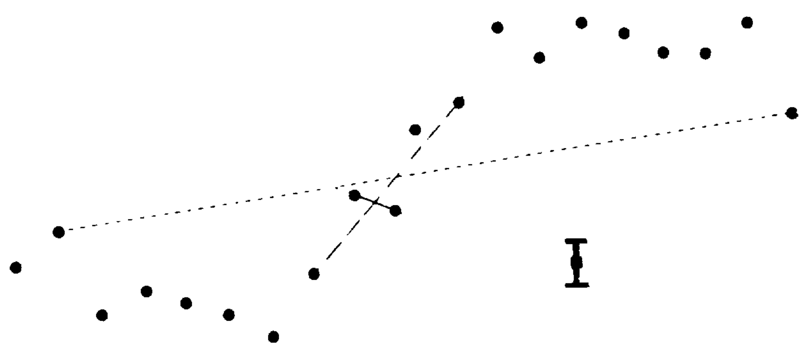

Fig. 2. Data profile over inclined edge embedded in "noise". Schematic error bounds are given at right. We want to locate the edge and determine its slope. The solid, long dashed, and and short dashed lines are slopes estimated from narrow, intermediate, and wide gradient determining operators respectively.

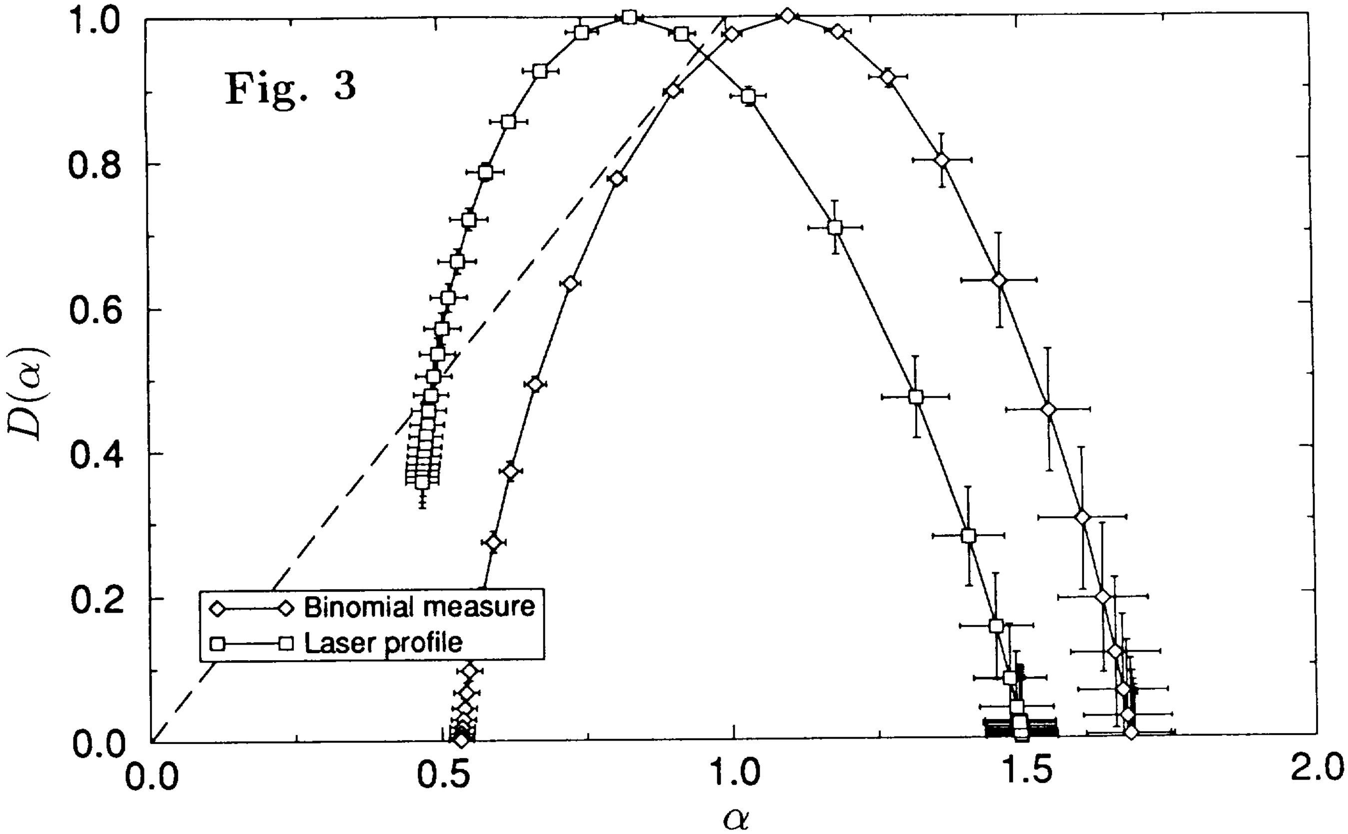
Fig. 3
1.0
0.8
0.6
0.4
0.2
0.0
$D(\alpha)$
0.0
0.5
1.0
1.5
2.0
α
Binomial measure
Laser profile

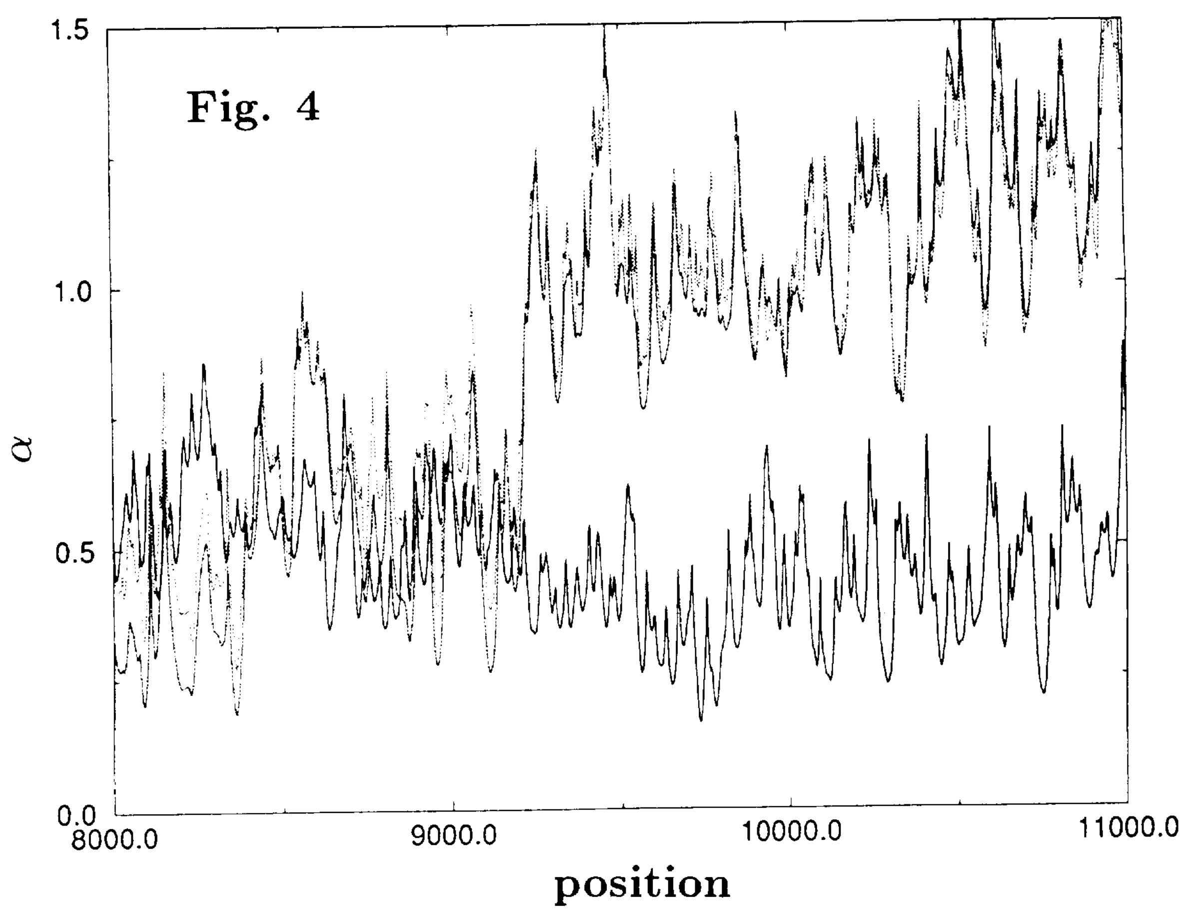
Fig. 4
1.5
1.0
0.5
0.0
α
8000.0
9000.0
10000.0
11000.0
position